IOPscience iopscience.iop.org

Home Search Collections Journals About Contact us My IOPscience

Powder neutron diffraction studies of Zn-doped magnetite

This article has been downloaded from IOPscience. Please scroll down to see the full text article.

1999 J. Phys.: Condens. Matter 11 2749

(http://iopscience.iop.org/0953-8984/11/13/011)

View the table of contents for this issue, or go to the journal homepage for more

Download details:
IP Address: 171.66.16.214
The article was downloaded on 15/05/2010 at 07:16

Please note that terms and conditions apply.

J. Phys.: Condens. Matter **11** (1999) 2749–2758. Printed in the UK PII: S0953-8984(99)99932-0

Powder neutron diffraction studies of Zn-doped magnetite

A Kozłowski†, Z Kąkol†, R Zalecki†, K Knight‡, J Sabol§ and J M Honig‖

† Department of Solid State Physics, University of Mining and Metallurgy, Kraków, Poland
‡ Rutherford Appleton Laboratory, ISIS, Chilton, UK
§ University of Wisconsin–Eau Claire, Eau Claire, WI, USA
‖ Department of Chemistry, Purdue University, West Lafayette, IN, USA

Received 4 December 1998

Abstract. We report on systematic neutron powder diffraction measurements of the temperature dependence of the crystal structure for the $Fe_{3-x}Zn_xO_4$ ($x < 0.036$) series. Time-of-flight data were collected on the spallation source ISIS (RAL, UK) between 4.2 and 270 K for samples showing different orders of the Verwey transition. The change of transition order is accompanied by the clear difference in the characteristic low temperature rhombohedral distortion. Namely, this distortion is independent of the dopant concentration for samples undergoing a first order Verwey transition, while the distortion for samples showing second order transition is much smaller and gradually diminishes with increasing Zn content. This distinct behaviour is linked to a change of atomic ordering from a well defined configuration for the first order regime to a dynamically changed arrangement for highly doped magnetite. This points to a close connection between the order of the Verwey transition and crystal lattice properties.

1. Introduction

The Verwey transition in magnetite at 120 K is a spectacular first-order phase transformation accompanied by the crystal symmetry change and an anomaly in several physical properties. It has been the object of interest for over 60 years and the reader is referred to [1–3] for representative literature reviews.

It is commonly believed that the transition is related to the iron cation valence instability. Below the transition temperature the distribution of Fe^{2+} and Fe^{3+} ions in octahedral (o) sites changes from dynamic disorder (electrons resonating on octahedral sites) to long-range order (LRO): the electrons tend to freeze out on selected octahedral positions. The number and the surroundings of the resonating electrons can be finely tuned by nonstoichiometry or doping with Zn and Ti, thus providing a means for the study of interactions leading to the transition [4, 5]. Despite the fact that all three kinds of defect introduce different perturbation to the system the properties of $Fe_{3(1-\delta)}O_4$, $Fe_{3-x}Ti_xO_4$ and $Fe_{3-x}Zn_xO_4$ are very similar. Specifically, as was proved by heat capacity and resistivity studies, the nature of the Verwey transition changes from first (I) to second (II) order when the degree of nonstoichiometry 3δ or concentration x exceeds $\sim$0.012; the transition disappears altogether when $3\delta = x > \sim 0.036$. For both the I and II order transition regions a universal linear T_V–$3\delta = x$ relation was found (see [2] and references therein).

For highly nonstoichiometric magnetite $\sim 0.012 < 3\delta < \sim 0.036$ it was even suggested [6] that the system may not exhibit a true phase transition. Despite this doubt, in the following text we will use working definition 'first'- and 'second'-order phase transitions to describe abrupt and smooth change in physical properties.

There is a long standing dispute as to the origin of the Verwey transition [7]. As pointed out by Anderson [8] every tetrahedron formed by the nearest-neighbour (○) sites of the spinel structure should be occupied by two Fe^{2+} and two Fe^{3+} ions, due to the strong Coulomb interaction between electrons. This strong nearest-neighbour Coulomb repulsion U_1 stabilizes the short-range order (SRO), but additional interactions are required to stabilize LRO. The energy U_2 needed to do this could be only a small fraction of the energy U_1; its origin is still a subject of dispute. Several mechanisms were proposed as a possible source for these interactions.

In our recent heat capacity measurements [2, 9, 10] we have found a clear difference between the data for first- and second-order samples. Namely, there is almost no shift in the baselines with doping above T_V, whereas below T_V the baselines of second-order specimens are higher than those of first order (see figure 1(a)). An alternative way of looking at the data is shown in figure 1(b), where the temperature dependence of the effective Debye temperature θ_D is presented. Note that below the transition θ_D is shifted upward by about 50 K for first-order samples, as compared to the values extrapolated from high temperatures, and that θ_D for second-order samples passes smoothly through the transition. A similar shift in Debye temperature for stoichiometric magnetite was also observed by Takai *et al* [11].

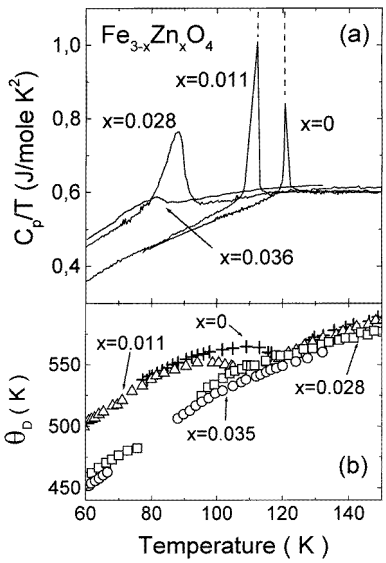

Figure 1. (a) C_p/T against T for $Fe_{3-x}Zn_xO_4$ exhibiting Verwey transitions of different order: $x = 0$ and 0.0110—first order, $x = 0.0280$ and $x = 0.036$—second order; (b) characteristic Debye temperature in the vicinity of the transition. Note that peaks were removed for clarity.

These differences were analysed in terms of various possible contributions to the heat capacity and attributed to a change of lattice elastic properties at T_V for first-order samples [9]. No such change is present in second-order specimens.

It is obvious that the lattice must be taken into account while describing the Verwey transition since this transformation is accompanied by a crystal symmetry change. In fact, some authors [12–14] have suggested an intimate connection between the Verwey transition and crystal lattice properties. In particular Honig and Spatek [14] proposed a microscopic model in which this transformation is driven by a change in the highly correlated electron system associated with local lattice deformations. Our heat capacity observations indicate that the change of the phase transition order may also be driven by the lattice dynamics.

We believe that one way to further highlight this problem and to supplement our heat capacity observations is to look at differences in the structures for slightly doped magnetite exhibiting the Verwey transition of different order at temperatures below and above the transition. Structure measurements were performed on the high resolution powder diffractometer (HRPD) at the pulsed spallation neutron source ISIS located at Rutherford Appleton Laboratory, UK.

Below, we first provide a short overview of the magnetite structure and describe the sample preparation procedure and diffraction measurements. The subsequent sections contain the presentation of the results and the discussion.

The crystalline structure of magnetite above the Verwey transition is well known to be the cubic inverse spinel represented by $(Fe^{3+})[Fe^{2+}, Fe^{3+}]O_4$, where parentheses ( ) denote tetrahedral (t) lattice site and brackets [ ], octahedral (o) lattice sites (figure 2(a)). The smallest cell of the spinel structure with cubic symmetry contains 32 oxygen ions that form an f.c.c. lattice belonging to the $Fd3m$ space group. This structure holds also for the high-temperature phase of Zn and Ti doped magnetite. The crystal structure of magnetite below the Verwey transition was found to be monoclinic (space group Cc) [15, 16], with the exception of the magnetoelectric effect measurements [17, 18] that suggested the breaking of the ac mirror plane symmetry, implying triclinic symmetry. However, it should be emphasized that all direct crystal structure measurements point to monoclinic structure as indicated by the characteristic features of the observed diffraction pattern [19]:

(i) a rhombohedral distortion of the cubic unit cell,
(ii) a doubling of the cell along the c-axis,
(iii) the existence of c-glide.

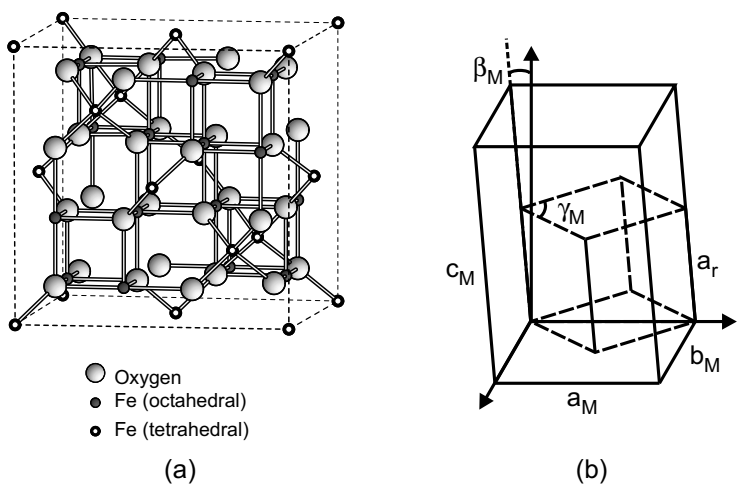

Figure 2. (a) High temperature spinel structure of magnetite; (b) relation between monoclinic (solid) and rhombohedrally distorted (dashed) unit cells.

The basis vectors a_M, b_M and c_M of the monoclinic unit cell roughly coincide with $[1\bar{1}0]$, [110] and [001] directions of the original cubic lattice, as shown in figure 2(b). The monoclinic c_M-axis is actually tilted $\sim 0.20^\circ$ away from the vertical towards the $-a_M$-direction (see again figure 2(b)), due to rhombohedral elongation along the $[\bar{1}11]$ or $[\bar{1}1\bar{1}]$ axes. The displacements of atoms comparing to cubic symmetry is reported to be of the order of 0.1 Å.

Although the low-temperature symmetry of magnetite is known there is a controversy about the particular prevailing cationic order. The original Verwey pattern [20] has been

disproved by neutron [15] and electron diffraction [16] as well as by NMR studies [21], but none of ten possible arrangements was experimentally proved (see e.g. [16] for the detailed discussion of those ten models).

The structural studies of Fe_3O_4 were not extended to nonstoichiometric or low-level doped magnetite, but it is tempting to interpret the Verwey transition and the striking similarities in physical properties of $Fe_{3(1-\delta)}O_4$, $Fe_{3-x}Ti_xO_4$ and $Fe_{3-x}Zn_xO_4$ ($x < 0.04$) below T_V as indicating the same change of structure as in pure magnetite. The present studies were in part designed to check this assumption.

2. Experimental details

In view of the small atomic displacements mentioned above our project required very high-precision measurements on very well characterized samples. Single-crystalline zinc ferrites, $Fe_{3-x}Zn_xO_4$ with small doping levels x, were grown from the melt by the cold crucible technique (skull melter) [22], at Purdue University, USA. The crystals were then subjected to subsolidus annealing under CO/CO_2 gas mixtures to establish the appropriate metal/oxygen ratio [23]. The actual composition and sample uniformity were checked using a microprobe electron analyser.

Neutron diffraction measurements were carried out on stoichiometric magnetite (Fe_3O_4) and four zinc ferrite ($Fe_{3-x}Zn_xO_4$) samples. Since the HRPD technique requires $\sim$1 cm^3 of a powder sample two to four individual single crystals of appropriate composition were pulverized (grain size 10–30 μm) to match this need. Such a procedure resulted in unavoidable Zn inhomogeneities, much larger than those encountered in individual single crystals. Stoichiometric magnetite and the sample with the mean composition $x = 0.0072 \pm 0.0020$ fall within the first-order transition range, while specimens with $x = 0.0185 \pm 0.0025$, $x = 0.0250 \pm 0.0025$ and $x = 0.0360 \pm 0.0030$ show transitions of the second order. The last one falls very close to the composition boundary beyond which no anomaly is encountered.

HRPD is a time-of-flight instrument (t-o-f) that provides very high resolution (up to $\Delta d/d = 4 \times 10^{-4}$), constant over a wide d-spacing range. It permits the observation of subtle symmetry changes in phase transition studies, and lattice parameter determinations, along with the potential for accurate structure refinements. In our case we have focused on the observation of the rhombohedral distortion and its changes at the transition. More precise structure refinements and the observation of subtle phenomena characteristic of monoclinic symmetry (such as (ii) and (iii) mentioned above) would require much longer data collection times. Our measurements were thus designed to investigate differences in the low-temperature lattice distortion between samples showing first- and second-order Verwey transitions.

The powder samples were mounted in rectangular vanadium sample holder supplied with two rhodium–iron thermometers, and a heater. The temperatures of the samples were stabilized by the temperature controller to within $\pm$0.2 K.

The t-o-f diffraction data were collected by the fixed angle back scattering detectors. The t-o-f range used was 20–130 ms corresponding to d-spacing of 0.6–2.6 Å. Under these experimental settings the diffraction data have an approximately constant resolution of $\Delta d/d = 8 \times 10^{-4}$. A more detailed description of the apparatus is presented elsewhere [24].

The temperature was scanned at intervals of 10 K (1 or 2 K in the region close to the transition). To cover the wide temperature range we have normally chosen short counting times of 10 min, sufficient for the evaluation of lattice parameters. To check for superlattice peaks we performed a 24 h run for Fe_3O_4 at 4.2 K and 3 h runs at selected temperatures below and above T_V for all other samples.

3. Results and discussion

Full profile Rietveld [25] refinements (modified for the t-o-f technique) were performed on all the data. For each sample at temperatures above T_V the best fit was obtained assuming cubic $Fd3m$ symmetry, in full agreement with the data reported for pure magnetite.

Low-temperature (below T_V) diffraction patterns for first-order samples (Fe_3O_4 and $x = 0.0072$) showed a clear splitting of $\langle hhh \rangle$ (with the intensity ratio 3:1) and $\langle hh0 \rangle$ (intensity ratio 1:1) cubic reflections which rapidly coalesce at the transition (see figure 3 for the $x = 0.0072$ data). This is again in agreement with literature reports concerning the rhombohedral elongation of the original cubic cell along the $\langle 111 \rangle$ direction. An attempt was made to refine the patterns based on the reported monoclinic symmetry. This, however, was only successful for the 24 h run for Fe_3O_4; for all other measurements the procedure did not converge, probably as a result of insufficient measuring time. For such short time spans, the intensity of some reflections characteristic of the monoclinic structure was of the order of the background signal. For example the $\langle 40\frac{1}{2} \rangle$ peak that should result from the doubling of the unit cubic cell in the [001] direction was visible only after at least 3 h of data collection (see figure 4). Consequently, we refined the low-temperature structure based on rhombohedral face centring $R\bar{3}m$ symmetry up to the transition temperature. The relation between this and the monoclinic structure is marked in figure 2(b); one can calculate monoclinic lattice parameters a_M, b_M, c_M and the angle β_M from the corresponding rhombohedral parameters a_r and γ_r, using the formulas:

$$a_M = \sqrt{2}a_r(1 + \cos\gamma_r)^{1/2}$$
$$b_M = \sqrt{2}a_r(1 - \cos\gamma_r)^{1/2}$$
$$c_M = 2a_r$$
$$\cos\beta_M = \sqrt{2}\cos\gamma_r(1 + \cos\gamma_r)^{1/2}.$$

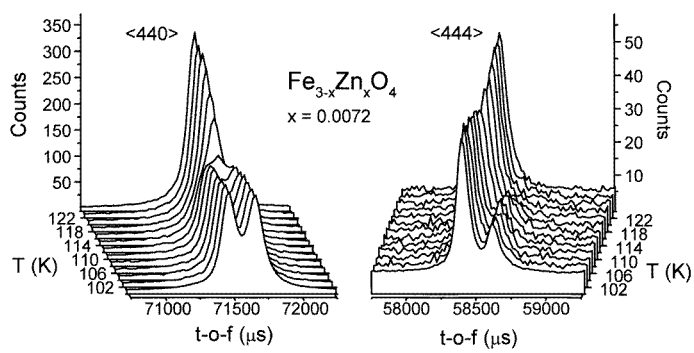

Figure 3. Temperature dependence of $\langle 440 \rangle$ and $\langle 444 \rangle$ peak splitting for the $Fe_{3-x}Zn_xO_4$, $x = 0.0072$ sample.

In the second-order regime, only the sample with lowest Zn concentration, $x = 0.0185$, showed a splitting of the $\langle hh0 \rangle$ and $\langle hhh \rangle$ low-temperature reflections. Two other samples, $x = 0.0250$ and $x = 0.0360$, show broadening of the relevant $\langle hhh \rangle$ and $\langle hh0 \rangle$ reflections, instead of splitting. The temperature dependence of full width at half maximum of the reflection, representing this broadening, is presented in figure 5 for $x = 0.0250$ and agrees with the occurrence of a continuous phase transition (in contrast to the temperature dependence of peak splitting for $x = 0.0072$, also shown in figure 5, in accordance with a first-order phase

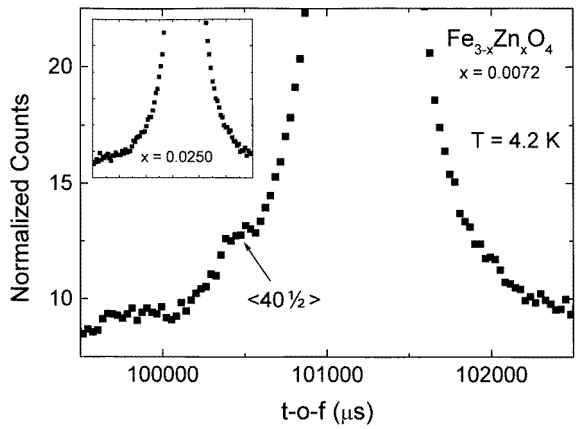

Figure 4. $\langle 40\frac{1}{2}\rangle$ satellite of $\langle 400\rangle$ peak reflecting doubling of the cubic c-axis for the $Fe_{3-x}Zn_xO_4$, $x = 0.0072$ sample.

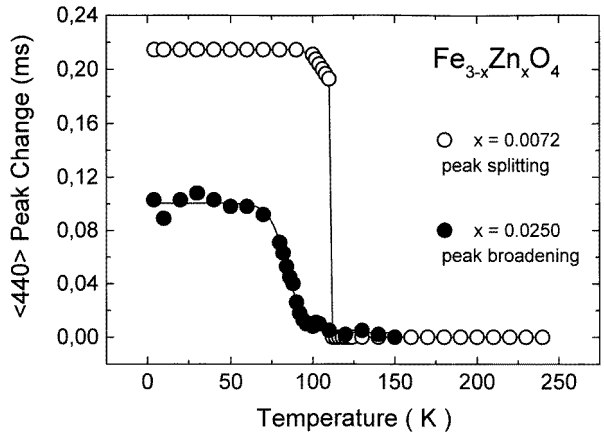

Figure 5. Comparison of $\langle 440\rangle$ reflection change at the transition for second-order sample (full width at half maximum FWHM change) with that observed in first-order samples (peak splitting).

transition). This time, even after 3 h measuring time we could not observe a $\langle 40\frac{1}{2}\rangle$ peak (inset in figure 4). It would probably require much longer measuring time since for second-order samples the intensities of the superlattice peaks are smaller [6].

Again, we refined the low-temperature structure based on the rhombohedral face centring $R\bar{3}m$ symmetry up to transition temperature. For high temperatures (above T_V) cubic symmetry was used for refinement.

The results of this refinement for all the samples are shown in figure 6 where the temperature dependence of the lattice parameters is presented; for first-order samples a changes abruptly at $T = T_V$, in contrast to second order, where lattice parameters pass smoothly through the transition region.

The most straightforward comparison of two regimes is displayed in figure 7, where $\langle 440\rangle$ reflections at $T = 4.2$ K for all samples are shown. The splitting of the $\langle 440\rangle$ reflections is almost identical for both first-order samples and much larger than that in the second-order regime where it gradually diminishes with increasing Zn concentration. The same trend is also

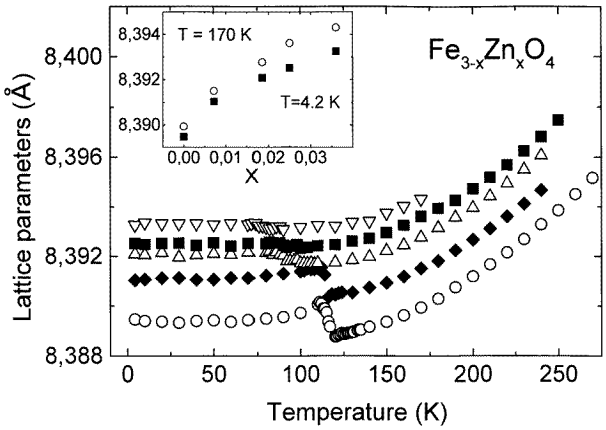

Figure 6. Temperature dependence of rhombohedral and cubic lattice parameters; ○—$x = 0$, ♦—$x = 0.0072$, △—$x = 0.0185$, ■—$x = 0.0250$, ▽—$x = 0.0360$. The inset shows lattice parameters against Zn concentration for selected temperature below (4.2 K) and above (170 K) the transition.

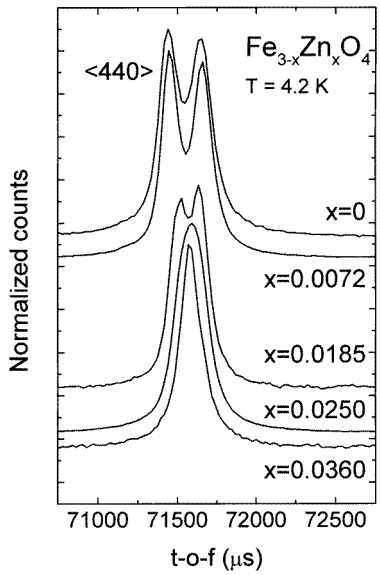

Figure 7. Comparison of ⟨440⟩ peak for first- and second-order samples at $T = 4.2$ K.

present in the ⟨444⟩ reflections. This feature is even better recognized in figure 8, where the β_M against Zn concentration at 4.2 K is presented. Apparently, we observe two distinct regimes, indicating that doped magnetite falls within two structurally different classes of materials.

The rhombohedral distortion β_M remains constant for all temperatures below T_V as presented in the β_M–T plot (figure 9). The data for first-order specimens nearly overlap and fall much above those for second-order samples. The inset shows a fit of $\beta_M \sim (1-T/T_V)^\alpha$ power law in the vicinity of the transition. Within the fitting error, we found the same exponent $\alpha \cong 1.3$ for first-order samples, while two different values of $\alpha = 0.55$ and $\alpha = 0.3$ were encountered for second-order samples with Zn content $x = 0.0185$ and $x = 0.0250$ respectively.

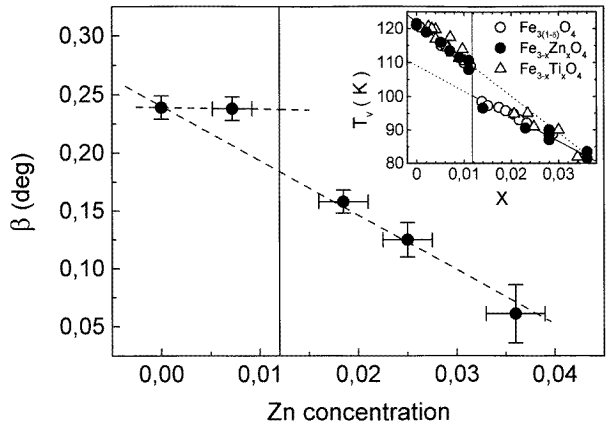

Figure 8. Monoclinic angle β_M against Zn concentration at $T = 4.2$ K. The inset shows variation of Verwey transition temperature against sample composition for $Fe_{3-x}Zn_xO_4$, $Fe_{3-x}Ti_xO_4$ and $Fe_{3(1-\delta)}O_4$.

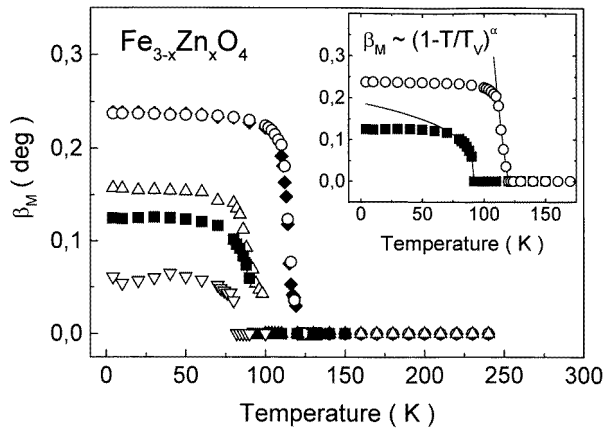

Figure 9. Temperature dependence of monoclinic angle β_M for first- and second-order samples; ○—$x = 0$, ◆—$x = 0.0072$, △—$x = 0.0185$, ■—$x = 0.0250$, ▽—$x = 0.0360$. The inset shows a fit of the $\beta_M \sim (1 - T/T_V)^\alpha$ power law in the vicinity of the transition.

The results of our measurements suggest that the lattice change under doping and/or temperature is different for first- and second-order samples. As stated in the introduction, the same behaviour has already been reported for Verwey temperature T_V dependence on composition and/or nonstoichiometry parameter (see inset in figure 8), and for heat capacity baselines (figure 1). Based on these results one notes that first- and second-order samples fall within two distinct universality classes. On the other hand, the compositional dependence of the lattice parameters at temperatures both below and above T_V (inset in figure 6) does not show any clear evidence of the transition or of the two regimes discussed above. This may mean that the electrostatic energy (Madelung energy) change at the Verwey transition is very subtle.

The conjecture that the energy difference between possible atomic arrangements in magnetite may be minute has already been recognized in the past. At high temperatures

carriers oscillate rapidly between energetically possible arrangements that satisfy the Anderson condition, leading to a strong short-range order. The entropy of this state is high. When the stoichiometric system cools down some stable, although still unknown, atomic pattern develops at T_V. Attempts were made to calculate this proper ionic order from electron correlation energy considerations [16, 26]. When only Coulomb repulsion between first- and second-nearest neighbours is taken into account [26] the most stable structure, though not realized in practice, is the Verwey original pattern, but the other configurations are very close to it in the energy scale [16, 26, 13], i.e. almost degenerate. Clearly, any small additional interaction may lift this Coulomb degeneracy and stabilize the proper charge order. Several authors suggest that this degeneracy is removed by electron–lattice interactions; our heat capacity and neutron results strongly support this conjecture. It was shown, however, that the electron hopping on the B sublattice (band structure effects) can also stabilize structures other than that proposed by Verwey (e.g. Mizoguchi structure as in [26]) to such an extent that electron–phonon coupling is not necessary for stabilization. Namely, a small change in the hopping (transfer) integral can force a different charge order to appear. As a consequence, we believe that whatever other interactions beyond Coulomb and electron–lattice are important, the system is close to an instability, characteristic for all strongly correlated systems. Consequently, the change of atomic distances, as achieved by doping beyond the 0.012 Zn concentration, may force the system to another low-temperature charge arrangement.

This other arrangement, occurring in second order, is either one of the stable arrangements listed in [16] and possibly still changing with further doping, or is a dynamic state where mobile electrons travel across different octahedral sites, preserving at the same time the monoclinic symmetry of the lattice, in contrast to the fully disordered state above T_V. To some extent this resembles the model proposed in [6], that in second-order nonstoichiometric magnetite the system breaks into domains, i.e. the LRO is missing below T_V.

The Verwey transition then represents a transformation from a highly degenerate high temperature state to either a well defined low-T ionic arrangement, as for first-order materials, or to a state with dynamically changing collection of atomic arrangements. In the first case the entropy change is considerable: two free energy curves for the low- and high-T regimes intersect, and the transition is first order. On the other hand, the much smaller entropy change for $x > 0.012$ may lead to a transition of second order.

Any atomic arrangement, stable or dynamic, is reflected in electronic properties, e.g. transport characteristics. Since, due to strong electron–lattice interactions, the carriers in magnetite are not bare electrons but small polarons [27, 28], the effective Coulomb interaction potential between these carriers depends on the lattice vibration spectrum [27]. Specific heat data show that for first-order Verwey transition this spectrum changes rapidly at T_V, which may result in a sudden increase of Coulomb repulsion: the system settles in an insulating, well characterized ionic state. For second-order samples, however, the dynamical atomic order, with a vibration spectrum similar to that at high T, does not lead to a pronounced change in Coulomb interactions: the boot-strap process possibly present in first-order materials does not take place.

This explanation would suggest that transport properties should also show distinct behaviour for first- and second-order samples. This is, in fact, what was observed, see e.g. [29]; but we also showed [29] that the composition dependence of the resistivity drop, $\Delta\rho$, at the transition changes smoothly across $x = 0.012$ both for doped (Ti and Zn) and nonstoichiometric samples. So, either the factor that governs this drop is not the one that determines the change of transition order, or this effect is more subtle and cannot be explained by such a simple considerations as above. In fact, transport effects involve hopping integrals, besides Coulomb repulsion energy [27] that may also change at T_V.

In summary, the present results show that there is a clear difference in lattice properties between first- and second-order samples below the transition temperature. In particular, the lattice distortion that develops at the transition is much larger for first- than for second-order samples. Moreover, it is nearly independent of the dopant concentration for $x < 0.012$, while it gradually diminishes with increasing Zn content in the second-order regime. Certainly, in the compositional range $0 < x < 0.036$, $Fe_{3-x}Zn_xO_4$ forms two structurally different classes of materials. This observation, together with our heat capacity data, points to a close connection between the Verwey transition and crystal lattice properties. In our interpretation we suggest that for the first-order regime one unique atomic and charge ordering develops below T_V, whereas in second order a dynamically changing arrangement is encountered. This may also explain the change of the transition character with doping.

Acknowledgments

This research was supported by the KBN-State Committee for Scientific Research grant No 2 P03B 036 14 and by the Faculty of Physics and Nuclear Techniques, University of Mining and Metallurgy. ZK, AK and RZ acknowledge support from the British Council and Rutherford Appleton Laboratory. JMH acknowledges support from NSF on grant DMR 96 12130 and JS acknowledges support from the Office of University Research, University of Wisconsin-Eau Claire.

References

[1] Shepherd J P, Koenitzer J W, Aragón R, Sandberg C J and Honig J M 1985 *Phys. Rev.* B **31** 1107
[2] Shepherd J P, Koenitzer J W, Aragón R, Spałek J and Honig J M 1991 *Phys. Rev.* B **43** 8461
[3] Aragón R, Rasmusen R J, Shepherd J P, Koenitzer J W and Honig J M 1988 *J. Magn. Magn. Mater.* **54–57** 1335
[4] Wang P, Kąkol Z, Wittenauer M and Honig J M 1990 *Phys. Rev.* B **42** 4553
[5] Kąkol Z, Sabol J, Stickler J and Honig J M 1992 *Phys. Rev.* B **46** 1975
[6] Aragón R, Gehring P M and Shapiro S M 1993 *Phys. Rev. Lett.* **70** 1635
[7] Tsuda N, Nasu K, Yanase A and Siratori K 1991 *Electronic Conduction in Oxides* (Berlin: Springer) ch 4.8.6 and references therein
[8] Anderson P W 1956 *Phys. Rev.* **102** 1008
[9] Kozłowski A, Kąkol Z, Kim D, Zalecki R and Honig J M 1996 *Phys. Rev.* B **54** 12 093
[10] Kozłowski A, Kąkol Z, Kim D, Zalecki R and Honig J M 1997 *Z. Anorg. (Allg.) Chem.* **623** 115
[11] Takai S, Yukikuni Y, Kawai H, Atake T and Sawaguchi E 1994 *Chem. Thermodyn.* **26** 1259
[12] Yamada Y, Wakabayashi N and Niclow N 1980 *Phys. Rev.* B **21** 4642
[13] Sokoloff J B 1976 *Phys. Rev.* B **13** 2003
[14] Honig J M and Spałek J 1992 *J. Solid State Chem.* **96** 115
[15] Shirane G, Chikazumi S, Akimitsu J, Chiba K, Matsui M and Fujii Y 1975 *J. Phys. Soc. Japan* **39** 947
[16] Zuo J M, Spence J C H and Petuskey W 1990 *Phys. Rev.* B **42** 8451
[17] Miyamoto Y and Chicazumi S 1988 *J. Phys. Soc. Japan* **57** 2040
[18] Miyamoto Y and Shindo M 1993 *J. Phys. Soc. Japan* **62** 1423
[19] Iizumi M, Koetzle T F, Shirane G, Chikazumi C, Matsui M and Todo S 1982 *Acta Crystallogr.* B **38** 2121
[20] Verwey E J W, Haaymann P W and Romeijn F C 1947 *J. Chem. Phys.* **15** 181
[21] Mizugouchi M 1978 *J. Phys. Soc. Japan* **44** 1501
Mizugouchi M 1978 *J. Phys. Soc. Japan* **44** 1512
[22] Harrison H R and Aragón R 1978 *Mater. Res. Bull.* **13** 1097
[23] Aragón R, Harrison H R, McCallister R H and Sandberg C J 1983 *J. Crystal Growth.* **61** 221
[24] Ibberson R M, David W F I and Knight K S 1992 *Rutherford Appleton Laboratory Report* RAL 92-031
[25] Rietveld H M 1969 *J. Appl. Crystallogr.* **2** 65
[26] Mishra S K and Satpathy S 1993 *Phys. Rev.* B **47** 5564
[27] Ihle D and Lorenz B 1986 *J. Phys. C: Solid State Phys.* **19** 5239
[28] Kozłowski A, Rasmussen R J, Sabol J E, Metcalf P and Honig J M 1993 *Phys. Rev.* B **48** 2057
[29] Kozłowski A, Metcalf P, Kąkol Z and Honig J M 1996 *Phys. Rev.* B **53** 15 113